

# On the Validity of the Born–Oppenheimer Separation and the Accuracy of Diagonal Corrections in Anharmonic Molecular Vibrations<sup>†</sup>

So Hirata\* and Edward B. Miller

Quantum Theory Project and The Center for Macromolecular Science and Engineering, Departments of Chemistry and Physics, University of Florida, Gainesville, Florida 32611-8435

Yu-ya Ohnishi

Department of Molecular Engineering, Graduate School of Engineering, Kyoto University, Nishikyo-ku, Kyoto 615-8510, Japan

Kiyoshi Yagi

Department of Applied Chemistry, School of Engineering, The University of Tokyo, Tokyo 113-8656, Japan

Received: April 12, 2009; Revised Manuscript Received: May 21, 2009

The energies and wave functions of several lowest-lying vibrational states of  $\text{FHF}^-$ ,  $\text{ClHCl}^-$ , and  $\text{BrHBr}^-$  have been computed by a finite-difference method with and without the Born–Oppenheimer (BO) separation between the heavy (halogen) and light (hydrogen) particle motion. The so-called diagonal BO correction (DBOC), which includes the effect of the heavy particles' kinetic energy operator acting on the light particles' wave functions, has also been made to the energies. The errors caused by the BO approximation are found to be remarkably small (ca.  $10^{-5}$  au) and can be systematically and effectively reduced by the DBOC except for states excited in the heavy particle motion. When the bare mass of the light particle is used instead of the reduced mass in the BO approximation and, therefore, the translational degrees of freedom are not correctly decoupled, the errors in the BO treatment become greater by a factor of 2–7. However, these additional errors are almost completely erased by the DBOC. Analytical and numerical results suggest that the remaining errors in the BO and DBOC treatments be proportional to  $\epsilon^1$  and  $\epsilon^2$ , where  $\epsilon$  is the mass ratio of the light to heavy particles, when the corrections are made to the potential energy surfaces and the wave functions for these surfaces are determined variationally. When the DBOC is applied in the first-order perturbation approximation, the remaining errors scale as  $\epsilon^{3/2}$ .

## I. Introduction

Accurate solutions of the Schrödinger equations of polyatomic molecules are hard to obtain because of their high dimensionality. A general and effective technique of tackling high-dimensional partial differential equations exists, however, and it is the approximate separation of variables. In computational quantum mechanics, this is invoked everywhere, but unquestionably the most important example is the Born–Oppenheimer (BO) separation<sup>1</sup> between the nuclear (vibrational, rotational, and translational) and electronic motion. A vast array of chemical properties (energies, spectra, reactions, etc.) of molecules containing even the lightest nuclei (protons) can be reproduced or predicted highly accurately within the BO approximation. Equally importantly, useful quantitative concepts of chemistry such as equilibrium molecular structures, potential energy hypersurfaces, Franck–Condon principles, and so forth are derived from this approximation.

Recently, considerable efforts have been devoted to *lifting* the BO separation between electrons and nuclei.<sup>2–7</sup> Given the success of the BO approximation, however, we find it equally or even more profitable to consider *introducing* an additional BO-like separation

between dynamical degrees of freedom with disparate mass or energy scales and study its validity. An ideal system for this study is a linear heavy–light–heavy molecule such as  $\text{FHF}^-$ ,  $\text{ClHCl}^-$ , or  $\text{BrHBr}^-$ , which has vibrations primarily involving hydrogen motion and a halogen–halogen stretching vibration that can be subject to a BO-like separation.<sup>8</sup> In this “second” BO approximation (as the usual BO separation between electrons and nuclei are also in operation), the two halogen atoms are held fixed in space and the hydrogen atom's three-dimensional equation of motion is solved initially. This is followed by the description of the halogen–halogen stretching motion in effective one-dimensional potentials defined by the hydrogen atom's vibrational energies. The heavy–light–heavy configuration of these molecules allows the three translational and two rotational degrees of freedom to be conveniently decoupled. Furthermore, the mass ratio ( $\epsilon$ ) of light to heavy particles in our vibrational problems is on the order of 0.1 as opposed to 0.0001 of electrons to nuclei, and therefore, the errors caused by the second BO separation should be quantified and analyzed relatively easily.

In this article, we shall show that, despite the very large mass ratio ( $\epsilon \approx 0.1$ ), the anharmonic vibrations involving primarily the halogen atoms and those involving the hydrogen atom can be treated separately, causing only small errors in  $\text{FHF}^-$  and even smaller, negligible errors in  $\text{ClHCl}^-$  and  $\text{BrHBr}^-$ . The errors caused by the BO approximation in the zero-point energies are shown both analytically and numerically to be asymptotically linear in  $\epsilon$ , contrary to the previous

<sup>†</sup> Part of the “Russell M. Pitzer Festschrift”.

\* To whom correspondence should be addressed. E-mail: hirata@tpf.ufl.edu.

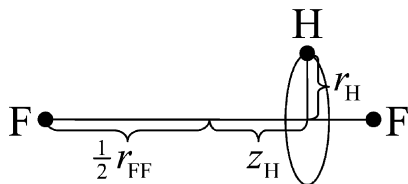


**Figure 1.** Cylindrical coordinates for  $\text{FHF}^-$ .

conclusions of Born and Oppenheimer<sup>1</sup> ( $\epsilon^{5/4}$ ) or that of Takahashi and Takatsuka<sup>9</sup> ( $\epsilon^{3/2}$ ). They are, however, consistent with the findings of Pino and Mujica<sup>10</sup> and Garashchuk et al.<sup>11</sup> in analytically solvable model problems. Furthermore, the BO errors can be reduced systematically and effectively by the diagonal BO corrections (DBOC)<sup>12</sup> except for states that are excited in the halogen–halogen stretching vibrations. The asymptote of the remaining errors is expected, mathematically, to be  $\epsilon^2$ , when the corrections are made to the potential energy surfaces and the wave functions for these surfaces are determined variationally. The numerical results are consistent with this analytical conclusion. When the DBOC is applied in the first-order perturbation approximation, the errors scale as  $\epsilon^{3/2}$ . Two ways of the BO separations (one using the bare hydrogen mass and the other the reduced hydrogen mass) and the corresponding DBOC have been examined, and the above conclusions are unaltered. This study strongly suggests that the BO separation has a broad range of applicability and should be applied to the dimensions that have been less explored by this general technique.

## II. Theory

This section and the next outline the definitions and algorithms of the BO and DBOC treatments using either reduced or bare mass of hydrogen, adopting  $\text{FHF}^-$  as a representative case.  $\text{ClHCl}^-$  and  $\text{BrHBr}^-$  can be treated in the same manner by making appropriate substitutions for the potential energy surface and the halogen masses.

$\text{FHF}^-$  is a linear equidistant molecule with four vibrational degrees of freedom: symmetric stretch, antisymmetric stretch, and doubly degenerate bend. Neglecting rovibration coupling (e.g., centrifugal distortion and Coriolis coupling), we can obtain their anharmonic frequencies and wave functions by solving the following vibrational Schrödinger equation (in atomic units) for a given potential energy surface,  $E_e(r_{\text{H}}, z_{\text{H}}, r_{\text{FF}})$ :

$$\left\{ -\frac{1}{2m_{\text{F}}'} \frac{\partial^2}{\partial r_{\text{FF}}^2} - \frac{1}{2m_{\text{H}}'} \nabla_{\text{H}}^2 + E_e(r_{\text{H}}, z_{\text{H}}, r_{\text{FF}}) \right\} \Psi(r_{\text{H}}, z_{\text{H}}, \varphi_{\text{H}}, r_{\text{FF}}) = E\Psi(r_{\text{H}}, z_{\text{H}}, \varphi_{\text{H}}, r_{\text{FF}}) \quad (1)$$

where  $E$  is the energy of a vibrational state,  $\Psi$  is the corresponding wave function, and  $m_{\text{F}}'$  and  $m_{\text{H}}'$  are reduced masses:  $m_{\text{F}}' = m_{\text{F}}/2$  and  $m_{\text{H}}' = 2m_{\text{F}}m_{\text{H}}/(2m_{\text{F}} + m_{\text{H}})$ , where  $m_{\text{F}}$  and  $m_{\text{H}}$  are the atomic masses of fluorine and hydrogen, respectively. The wave function is expressed in terms of the F–F distance  $r_{\text{FF}}$  and the hydrogen position  $(r_{\text{H}}, \varphi_{\text{H}}, z_{\text{H}})$  in the cylindrical coordinates anchored at the midpoint of the two fluorine atoms (Figure 1).  $E_e$  does not depend on the angle  $\varphi_{\text{H}}$ . In eq 1 and thereafter, the subscripts e, H, and F (or FF) refer to energies and wave functions of electrons, the hydrogen atom, and the fluorine atoms, respectively. The translational and rotational degrees of freedom have been removed from eq 1 except that, when  $r_{\text{H}} > 0$ , the molecule is bent and the four dynamical degrees of freedom under consideration consist of three vibrational and one rotational degree of freedom.

The question we ask in this study is how accurate the BO-like separation is between the hydrogen coordinates  $(r_{\text{H}}, \varphi_{\text{H}}, z_{\text{H}})$  and the fluorine coordinate  $(r_{\text{FF}})$  in solving eq 1. Unlike the usual BO separation between electrons and nuclei where the mass ratio is on the order of 0.0001, the mass ratio ( $\epsilon = m_{\text{H}}/m_{\text{F}}' \approx m_{\text{H}}'/m_{\text{F}}'$ ) in this purely vibrational problem is about 0.1. A difference between the solutions of eq 1 with and without the BO separation should, therefore, be greater and more precisely estimated. The comparison should give us a quantitative insight into the accuracy of the BO approximation in vibrations and, by extension, that of the BO approximation between electrons and nuclei, which is much harder to quantify.

The BO approximation consists in the forced factorization of the total wave function as follows:

$$\Psi(r_{\text{H}}, z_{\text{H}}, \varphi_{\text{H}}, r_{\text{FF}}) \approx \chi(r_{\text{H}}, z_{\text{H}}, \varphi_{\text{H}}; r_{\text{FF}}) \xi(r_{\text{FF}}) \quad (2)$$

where  $\chi(r_{\text{H}}, z_{\text{H}}, \varphi_{\text{H}}; r_{\text{FF}})$  is the vibrational wave function of the hydrogen atom's motion and  $\xi(r_{\text{FF}})$  is that of the fluorine atoms' motion. The hydrogen vibrational wave function  $\chi$  is a function of  $r_{\text{H}}$ ,  $z_{\text{H}}$ , and  $\varphi_{\text{H}}$  and depends parametrically on  $r_{\text{FF}}$  (the dynamical variables and parameters are separated by a semicolon). It is the solution of the three-dimensional partial differential equation

$$\left\{ -\frac{1}{2m_{\text{H}}'} \nabla_{\text{H}}^2 + E_e(r_{\text{H}}, z_{\text{H}}, r_{\text{FF}}) \right\} \chi(r_{\text{H}}, z_{\text{H}}, \varphi_{\text{H}}; r_{\text{FF}}) = E_{\text{eH}}(r_{\text{FF}}) \chi(r_{\text{H}}, z_{\text{H}}, \varphi_{\text{H}}; r_{\text{FF}}) \quad (3)$$

Note that the reduced hydrogen mass  $m_{\text{H}}'$  is used in light of the original Hamiltonian in eq 1. The only approximation is, therefore, the factorization in eq 2. However, the BO approximation in electronic structure theory involves another assumption in addition to eq 2, which is the use of  $m_{\text{H}}$  in the place of  $m_{\text{H}}'$ . We shall examine both equations: eq 3 and that in which  $m_{\text{H}}'$  is replaced by  $m_{\text{H}}$  (see below).

In the cylindrical coordinates, the Laplacian is expressed as

$$\nabla_{\text{H}}^2 = \frac{\partial^2}{\partial r_{\text{H}}^2} + \frac{1}{r_{\text{H}}} \frac{\partial}{\partial r_{\text{H}}} + \frac{1}{r_{\text{H}}^2} \frac{\partial^2}{\partial \varphi_{\text{H}}^2} + \frac{\partial^2}{\partial z_{\text{H}}^2} \quad (4)$$

Since the potential  $E_e(r_{\text{H}}, z_{\text{H}}, r_{\text{FF}})$  is axially symmetric,  $\chi$  can be written exactly in the factored form:

$$\chi(r_{\text{H}}, z_{\text{H}}, \varphi_{\text{H}}; r_{\text{FF}}) = \zeta(r_{\text{H}}, z_{\text{H}}; r_{\text{FF}}) \frac{\exp(-ik\varphi_{\text{H}})}{\sqrt{2\pi}} \quad (5)$$

where  $k$  is a quantum number that can take any integer value. The angular momentum of the hydrogen atom's rotational motion around the molecular axis is  $k$  au. The function  $\zeta$  satisfies the two-dimensional partial differential equation

$$\begin{aligned} -\frac{1}{2m_{\text{H}}'} \left( \frac{\partial^2}{\partial r_{\text{H}}^2} + \frac{1}{r_{\text{H}}} \frac{\partial}{\partial r_{\text{H}}} - \frac{k^2}{r_{\text{H}}^2} + \frac{\partial^2}{\partial z_{\text{H}}^2} \right) \zeta(r_{\text{H}}, z_{\text{H}}; r_{\text{FF}}) + \\ E_e(r_{\text{H}}, z_{\text{H}}, r_{\text{FF}}) \zeta(r_{\text{H}}, z_{\text{H}}; r_{\text{FF}}) \\ = E_{\text{eH}}(r_{\text{FF}}) \zeta(r_{\text{H}}, z_{\text{H}}; r_{\text{FF}}) \end{aligned} \quad (6)$$

where the coupling between  $r_H$  and  $z_H$  is strong and no further approximate separation of variables should be introduced. This equation was also considered by Lohr and Sloboda<sup>8</sup> previously. The singularities in the Laplacian ( $1/r_H$  and  $1/r_H^2$ ) require that

$$\left. \frac{\partial \zeta(r_H, z_H; r_{FF})}{\partial r_H} \right|_{r_H=0} = 0 \quad (7)$$

for  $k = 0$  and

$$\left. \frac{\partial \zeta(r_H, z_H; r_{FF})}{\partial r_H} \right|_{r_H=0} = a \quad (8)$$

for  $k = 1$ , where  $a$  is a nonzero constant. The function  $\zeta$  can be assumed real and normalized as

$$\iint dr_H dz_H r_H |\zeta(r_H, z_H; r_{FF})|^2 = 1 \quad (9)$$

The hydrogen atom’s vibrational energies  $E_{eH}(r_{FF})$  depend parametrically on  $r_{FF}$  and serve as an effective one-dimensional potential in a partial differential equation for  $\xi$ . In the approximation that we refer to as “BO (reduced hydrogen mass)”, we solve

$$\left\{ -\frac{1}{2m'_F} \frac{\partial^2}{\partial r_{FF}^2} + E_{eH}(r_{FF}) \right\} \xi^{BO}(r_{FF}) = E^{BO} \xi^{BO}(r_{FF}) \quad (10)$$

and compare  $E^{BO}$  with  $E$ . If we instead minimize an expectation value of the Hamiltonian of eq 1 in the wave function  $\chi \xi$  by varying  $\xi$ , we arrive at the following equation:

$$\left\{ -\frac{1}{2m'_F} \frac{\partial^2}{\partial r_{FF}^2} - \frac{U(r_{FF})}{m'_F} \frac{\partial}{\partial r_{FF}} - \frac{V(r_{FF})}{2m'_F} + E_{eH}(r_{FF}) \right\} \xi^{DBOC}(r_{FF}) = E^{DBOC} \xi^{DBOC}(r_{FF}) \quad (11)$$

with

$$U(r_{FF}) = \iint dr_H dz_H r_H \zeta(r_H, z_H; r_{FF}) \frac{\partial \zeta(r_H, z_H; r_{FF})}{\partial r_{FF}} \quad (12)$$

$$V(r_{FF}) = \iint dr_H dz_H r_H \zeta(r_H, z_H; r_{FF}) \frac{\partial^2 \zeta(r_H, z_H; r_{FF})}{\partial r_{FF}^2} \quad (13)$$

It is, however, noticed that  $U(r_{FF}) = 0$  because of eq 9. Equation 11 is, therefore, simplified to

$$\left\{ -\frac{1}{2m'_F} \frac{\partial^2}{\partial r_{FF}^2} + E_{eH}^{DBOC}(r_{FF}) \right\} \xi^{DBOC}(r_{FF}) = E^{DBOC} \xi^{DBOC}(r_{FF}) \quad (14)$$

where

$$E_{eH}^{DBOC}(r_{FF}) = E_{eH}(r_{FF}) - \frac{V(r_{FF})}{2m'_F} \quad (15)$$

which corresponds to the so-called “adiabatic” potential. We refer to this calculation as “DBOC (reduced hydrogen mass)” in the following. One can estimate the difference  $E^{DBOC} - E^{BO}$  accurately by the first-order perturbation theory also:

$$E^{DBOC} \approx E^{BO} - \frac{1}{2m'_F} \int dr_{FF} V(r_{FF}) |\xi^{BO}(r_{FF})|^2 \equiv \bar{E}^{DBOC} \quad (16)$$

We can begin with the following equation to study the same dynamics defined by eq 1:

$$\left\{ -\frac{1}{2m'_F} \frac{\partial^2}{\partial r_{FF}^2} - \frac{1}{2m'_{CM}} \nabla_{CM}^2 - \frac{1}{2m_H} \nabla_H^2 + E_e(r_H, z_H, r_{FF}) \right\} \tilde{\Psi}(r_H, z_H, \varphi_H, r_{FF}, \mathbf{r}_{CM}) = \tilde{E} \tilde{\Psi}(r_H, z_H, \varphi_H, r_{FF}, \mathbf{r}_{CM}) \quad (17)$$

where  $\mathbf{r}_{CM}$  is the center of mass (CM) of the two fluorine atoms,  $r_{FF}$  is the distance between the two, and the hydrogen position is in cylindrical coordinates anchored at the CM. The total ( $m'_{CM} = 2m_F$ ) and reduced ( $m'_F = m_F/2$ ) masses of the two fluorine atoms and the bare mass of the hydrogen atom ( $m_H$ ) are used. We distinguish quantities in eq 17 from the similar quantities in eq 1 by tildes to underscore the fact that they are numerically different. We introduce an approximation in the wave function, which reads

$$\tilde{\Psi}(r_H, z_H, \varphi_H, r_{FF}, \mathbf{r}_{CM}) \approx \tilde{\chi}(r_H, z_H, \varphi_H; r_{FF}, \mathbf{r}_{CM}) \tilde{\xi}(r_{FF}) \times \exp(-i\tilde{\mathbf{k}} \cdot \mathbf{r}_{CM}) \quad (18)$$

where the exponential factor describes the translational motion of the CM with the linear momentum  $\tilde{\mathbf{k}}$ . The rotational motion of the F–F skeleton is again suppressed because we include only one internal coordinate  $r_{FF}$  in the above. Because of the axial symmetry of the potential  $E_e$ , we find

$$\tilde{\chi}(r_H, z_H, \varphi_H; r_{FF}, \mathbf{r}_{CM}) = \tilde{\zeta}(r_H, z_H; r_{FF}, \mathbf{r}_{CM}) \frac{\exp(-ik\varphi_H)}{\sqrt{2\pi}} \quad (19)$$

where the quantum number  $k$  has the same meaning as before. The two-dimensional function  $\tilde{\zeta}$  must satisfy

$$\begin{aligned} & -\frac{1}{2m_H} \left( \frac{\partial^2}{\partial r_H^2} + \frac{1}{r_H} \frac{\partial}{\partial r_H} - \frac{k^2}{r_H^2} + \frac{\partial^2}{\partial z_H^2} \right) \tilde{\zeta}(r_H, z_H; r_{FF}, \mathbf{r}_{CM}) + \\ & E_e(r_H, z_H, r_{FF}) \tilde{\zeta}(r_H, z_H; r_{FF}, \mathbf{r}_{CM}) = \tilde{E}_{eH}(r_{FF}) \tilde{\zeta}(r_H, z_H; r_{FF}, \mathbf{r}_{CM}) \end{aligned} \quad (20)$$

where we have used the obvious fact that  $E_e$  and  $\tilde{E}_{eH}$  are translationally invariant. Notice that the bare mass of hydrogen  $m_H$  is used in the above equation. Therefore, this closely

resembles the BO approximation in usual electronic structure calculations, where the positions of the heavy particles (nuclei) are held fixed in space and *bare* electron masses are used in the electronic Hamiltonian. This is in contrast to eq 6, where both light and heavy particle motion is described in the relative coordinates and reduced masses are used.

The energies and wave functions of the heavy particle motion are obtained by solving the following one-dimensional partial differential equation for  $\xi$ :

$$\left\{ -\frac{1}{2m'_F} \frac{\partial^2}{\partial r_{FF}^2} + \tilde{E}_{eH}(r_{FF}) \right\} \xi^{\text{BO}}(r_{FF}) = \tilde{E}^{\text{BO}} \xi^{\text{BO}}(r_{FF}) \quad (21)$$

which we refer to as “BO (bare hydrogen mass)”. With diagonal corrections, that is, “DBOC (bare hydrogen mass)”, the equation to be solved is

$$\left\{ -\frac{1}{2m'_F} \frac{\partial^2}{\partial r_{FF}^2} - \frac{\tilde{V}(r_{FF})}{2m'_F} - \frac{\tilde{W}(r_{FF})}{2m'_{CM}} + \tilde{E}_{eH}(r_{FF}) \right\} \xi^{\text{DBOC}}(r_{FF}) = \tilde{E}^{\text{DBOC}} \xi^{\text{DBOC}}(r_{FF}) \quad (22)$$

where

$$\tilde{V}(r_{FF}) = \iint dr_H dz_H r_H \tilde{\xi}(r_H, z_H; r_{FF}, \mathbf{r}_{CM}) \frac{\partial^2 \tilde{\xi}(r_H, z_H; r_{FF}, \mathbf{r}_{CM})}{\partial r_{FF}^2} \quad (23)$$

$$\tilde{W}(r_{FF}) = \iint dr_H dz_H r_H \tilde{\xi}(r_H, z_H; r_{FF}, \mathbf{r}_{CM}) \nabla_{CM}^2 \tilde{\xi}(r_H, z_H; r_{FF}, \mathbf{r}_{CM}) \quad (24)$$

Because the hydrogen position is relative to the fluorine atoms' CM, to evaluate  $\tilde{W}(r_{FF})$ , we can use the relation

$$\nabla_{CM}^2 \tilde{\xi}(r_H, z_H; r_{FF}, \mathbf{r}_{CM}) = \nabla_H^2 \tilde{\xi}(r_H, z_H; r_{FF}, \mathbf{r}_{CM}) \quad (25)$$

and the computational machinery similar to the one for solving eq 20. Equation 23 corrects the error caused by the approximate separation of variables introduced in eq 18. Equation 24, on the other hand, addresses the error arising from the additional tacit approximation in the BO scheme, namely, the so-called “reduced mass error” as pointed out by Handy and Lee<sup>12</sup> and discussed extensively by Kutzelnigg.<sup>13,14</sup> See also Garashchuk et al.<sup>11</sup> on this issue in the context of an analytically solvable model.

### III. Computational Details and Results

Two-dimensional partial differential eqs 6 and 20 were solved by a finite-difference method on an evenly spaced  $21 \times 41$  rectangular  $r_H$ – $z_H$  grid at the interval of 5 pm. The second and first derivatives were evaluated by three- and two-point formulas, respectively:

$$\frac{\partial^2 f(r, z)}{\partial r^2} \Big|_{r, z_j} \approx \frac{f(r_{i+1}, z_j) - 2f(r_i, z_j) + f(r_{i-1}, z_j)}{\Delta r^2} \quad (26)$$

$$\frac{\partial f(r, z)}{\partial r} \Big|_{r, z_j} \approx \frac{f(r_{i+1}, z_j) - f(r_{i-1}, z_j)}{2\Delta r} \quad (27)$$

At  $r_H = 0$ , the singular (i.e., the second and third) terms in the kinetic energy operator of eqs 6 and 20 were simply omitted. This was justified because they must both vanish when  $k = 0$  and they must cancel with each other when  $k \geq 1$ . The resulting wave functions were found to satisfy the conditions of eqs 7 and 8. The  $861 \times 861$  Hamiltonian matrix was diagonalized, and all eigenvalues and the corresponding right ( $\zeta$  or  $\tilde{\zeta}$ ) and left ( $r_H \zeta$  or  $r_H \tilde{\zeta}$ ) eigenvectors were collected.

The eigenvalues and eigenvectors of three of these states were recorded at each point of the  $r_{FF}$  grid in the range of 170–310 pm at the interval of 2.5 pm (57 points) for  $\text{FHF}^-$ . The corresponding ranges in  $\text{ClHCl}^-$  and  $\text{BrHBr}^-$  were 252.5–435 pm at the interval of 1.25 pm (147 points) and 287.5–450 pm at the interval of 1.25 pm (131 points), respectively. The first state considered was the lowest root  $\zeta_0$  with  $k = 0$  (the zero-point vibration of the hydrogen). The wave function of this state in  $\text{FHF}^-$  at  $r_{FF} = 230$  pm is shown in Figure 2 along with the two-dimensional slice of the potential energy surface,  $E_e(r_H, z_H, r_{FF})$ . The second state considered was the second lowest root  $\zeta_1$  with  $k = 0$ , which corresponds to the antisymmetric stretch (Figure 3). Its wave function is characterized by a nodal plane perpendicular to the F–F axis. The third state is the lowest root  $\zeta_0$  with  $k = 1$  and is one of the degenerate bending vibrations (the counterpart is with  $k = -1$ ). Linear combinations of the complex wave functions of the degenerate states look like Cartesian  $p$ -type orbitals perpendicular to the F–F axis (Figure 4). As expected from eq 7, the wave functions in Figures 2 and 3 have vanishing first derivatives on the F–F axis. The wave function in Figure 4 vanishes on the same axis, satisfying eq 8. The same set of states in  $\text{ClHCl}^-$  and  $\text{BrHBr}^-$  was examined.

Figures 5 and 6 illustrate the  $\zeta_0$  ( $k = 0$ ) wave function of  $\text{FHF}^-$  at rather short (170 pm) and long (270 pm) F–F distances, respectively. At the short F–F distance, the hydrogen atom in its lowest-energy vibrational state can hardly exist at the midpoint of the F–F axis and the zero-point wave function becomes a torus (note our use of the cylindrical coordinates). At the long F–F distance, in contrast, the hydrogen atom experiences a double-well potential and its zero-point wave function consists of two well-separated disks. These observations

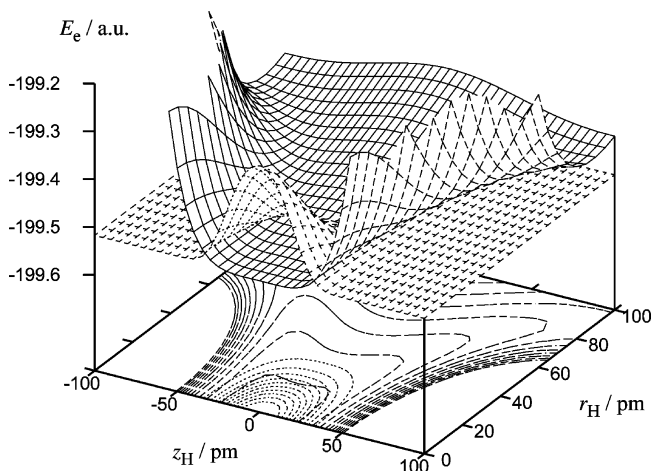


**Figure 2.** Potential energy surface,  $E_e$ , of  $\text{FHF}^-$  (surface drawn with solid curves and contours with broken curves) and the wave function  $\zeta_0$  with  $k = 0$  (surface drawn with broken curves and contours with dotted curves) at  $r_{FF} = 230$  pm.

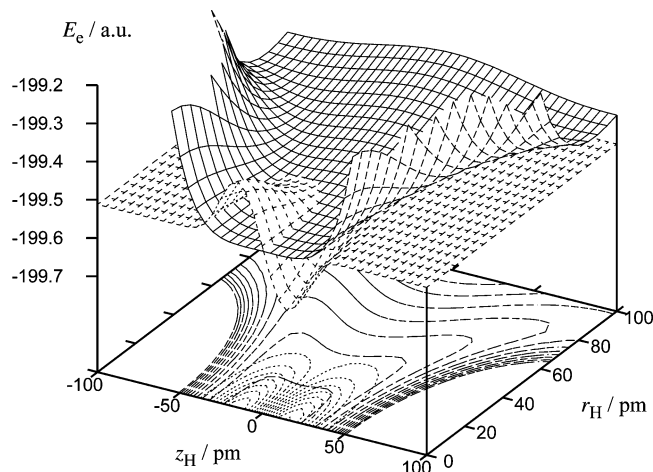


Figure 3. Same as Figure 2, but for  $\zeta_1$  with  $k = 0$ .

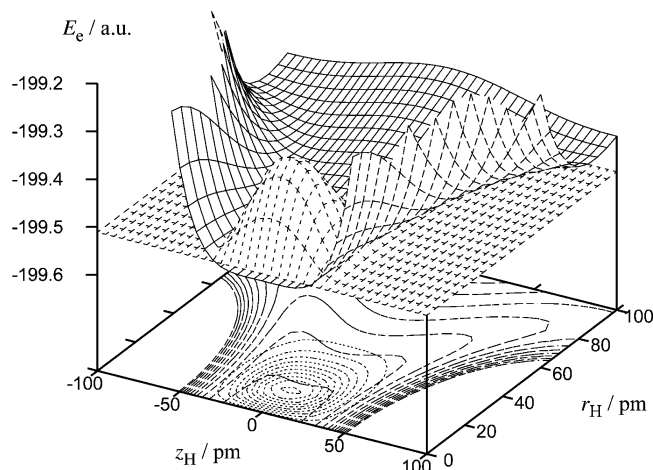


Figure 4. Same as Figure 2, but for  $\zeta_0$  with  $k = 1$ .

underscore the complex  $r_{\text{FF}}$  dependence of even the zero-point wave function of the hydrogen motion and the strong anharmonic coupling of all vibrational modes.<sup>15–17</sup>

The eigenvalues of these three states as functions of  $r_{\text{FF}}$  are plotted in Figure 7 (solid curves) for  $\text{FHF}^-$ . They serve as the effective potential energy curves ( $E_{\text{eH}}$  in eq 10 or  $\tilde{E}_{\text{eH}}$  in eq 21) for the F–F stretch. The DBOC to the effective potentials was computed according to eq 13 or eqs 23 and 24 and is shown in Figure 7 as broken curves (the magnitudes of the corrections are exaggerated in the figure). These corrections involve the differentiation of the wave functions  $\zeta(r_{\text{H}}, z_{\text{H}}; r_{\text{FF}})$  or  $\tilde{\zeta}(r_{\text{H}}, z_{\text{H}}; r_{\text{FF}}, \mathbf{r}_{\text{CM}})$  with respect to  $r_{\text{FF}}$ . To evaluate them correctly, these wave functions were made to be real, normalized according to eq 9, and phase-matched across the entire domain of  $r_{\text{FF}}$ . The fact that  $\zeta_0$  ( $k = 0$ ) and  $\zeta_1$  ( $k = 0$ ) curves merge into one curve at large values of  $r_{\text{FF}}$  is a result of the double-well nature of the potential (Figure 6), whose lowest root becomes doubly degenerate as the two wells are separated from each other.

In addition, the unapproximated (non-BO) Schrödinger eq 1 was solved for  $E$  by Davidson's trial vector algorithm.<sup>18</sup> Although eq 1 is four-dimensional, the angular ( $\varphi_{\text{H}}$ ) dependence can still be separated exactly because of the axial symmetry of the potential,  $E_{\text{e}}$ , and the problem is thus computationally only three-dimensional. The representations of the operators and the potential energy surface were made identical. Namely, the same cylindrical grids of sizes  $21 \times 41 \times 57$  for  $\text{FHF}^-$ ,  $21 \times 41 \times 147$  for  $\text{ClHCl}^-$ , and  $21 \times 41 \times 131$  for  $\text{BrHBr}^-$  were used to

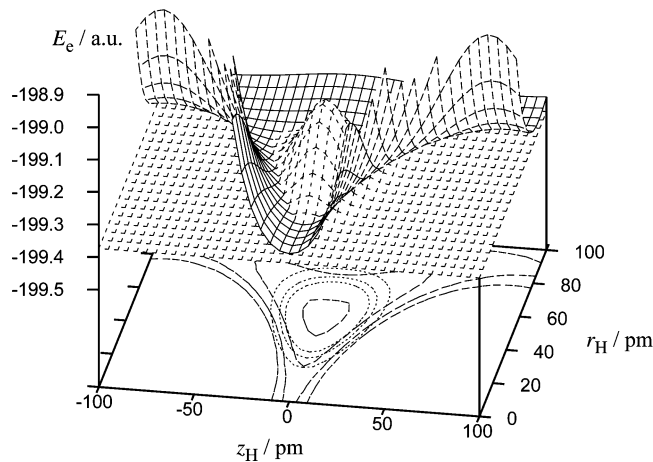


Figure 5. Same as Figure 2 with  $r_{\text{FF}} = 170$  pm.

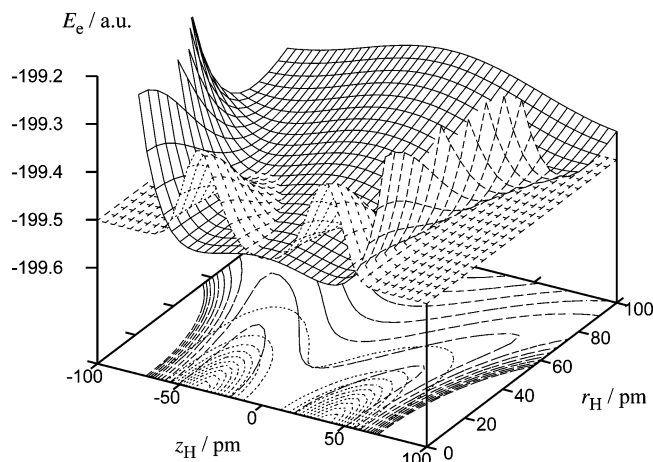


Figure 6. Same as Figure 2 with  $r_{\text{FF}} = 270$  pm.

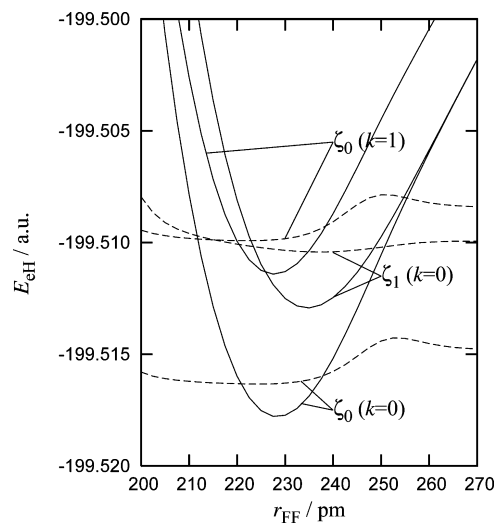


Figure 7. Potential energy curves in the BO (reduced hydrogen mass) approximation,  $E_{\text{eH}}$  (solid curves), and the DBOC,  $E_{\text{eH}}^{\text{DBOC}} - E_{\text{eH}}$  (broken curves; magnified by 10 times and relative to the minimum energies of the corresponding states).

support the potential energy surfaces, and the first and second derivatives were evaluated by the same two- and three-point finite-difference formulas, respectively. Therefore, any errors associated with these approximations should affect both the BO ( $E^{\text{BO}}$  and  $E^{\text{DBOC}}$ ) and non-BO ( $E$ ) calculations equally. The results of these calculations should be rigorously comparable with one another, and therefore, the errors introduced solely by

**TABLE 1: Energies (in au) of the Vibrational States of FHF<sup>-</sup>, ClHCl<sup>-</sup>, and BrHBr<sup>-</sup> and the Errors (in 10<sup>-6</sup> au) in the Energies Obtained by Employing the BO Approximation with and without the DBOC**

state <sup>a</sup>	root <sup>b</sup>	exact	reduced mass		bare mass		
			BO	DBOC	BO	DBOC	
FHF <sup>-</sup>							
(000)	$\zeta_0\xi_0$ ( $k=0$ )	-199.516292	-27	+7	-149	+4	
(100)	$\zeta_0\xi_1$ ( $k=0$ )	-199.513637	-27	+26	-149	+23	
(001)	$\zeta_1\xi_0$ ( $k=0$ )	-199.511488	-51	+9	-248	+7	
(010)	$\zeta_0\xi_0$ ( $k=1$ )	-199.509859	-32	+9	-233	+11	
ClHCl <sup>-</sup>							
(000)	$\zeta_0\xi_0$ ( $k=0$ )	-919.676878	-36	+7	-76	+7	
(100)	$\zeta_0\xi_1$ ( $k=0$ )	-919.675797	-40	+18	-83	+18	
(001)	$\zeta_1\xi_0$ ( $k=0$ )	-919.675482	-40	+4	-98	+4	
(010)	$\zeta_0\xi_0$ ( $k=1$ )	-919.673158	-49	+8	-115	+9	
BrHBr <sup>-</sup>							
(000)	$\zeta_0\xi_0$ ( $k=0$ )	-5145.451329	-26	+4	-42	+4	
(100)	$\zeta_0\xi_1$ ( $k=0$ )	-5145.450788	-6	+32	-11	+32	
(001)	$\zeta_1\xi_0$ ( $k=0$ )	-5145.450458	-19	+2	-41	+1	
(010)	$\zeta_0\xi_0$ ( $k=1$ )	-5145.448197	-26	+4	-52	+4	

<sup>a</sup> The quantum numbers of the symmetric stretch, bend, and antisymmetric stretch. <sup>b</sup> In the bare-mass calculations,  $\zeta$  and  $\xi$  should be understood to mean  $\tilde{\zeta}$  and  $\tilde{\xi}$ , respectively.

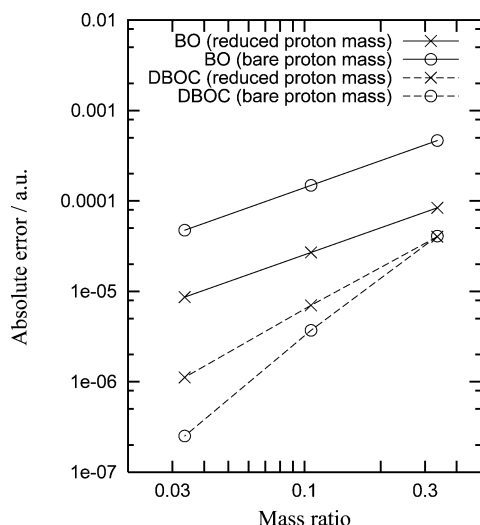


**Figure 8.** Absolute errors (in au) in the energies of the zero-point vibrational state of FHF<sup>-</sup> computed in the BO approximations with and without the DBOC plotted as functions of the mass ratio  $m_{\text{H}}/m_{\text{F}}$ . Both axes use logarithmic scales.

the BO approximation can be quantified. We refer to the energies  $E$  obtained by these non-BO calculations as “exact” in this article.

The results of the BO and DBOC calculations based on the reduced and bare hydrogen masses are compared with the exact results for four low-lying vibrational states in Table 1. Figure 8 plots the absolute values of the deviations in the BO and DBOC results from the corresponding exact values at three different fluorine masses:  $(10)^{1/2}m_{\text{F}}$ ,  $(1)^{1/2}m_{\text{F}}$ ,  $(0.1)^{1/2}m_{\text{F}}$ . Figures 9 and 10 are the same plots for ClHCl<sup>-</sup> ( $(10)^{1/2}m_{\text{Cl}}$ ,  $(1)^{1/2}m_{\text{Cl}}$ ,  $(0.1)^{1/2}m_{\text{Cl}}$ ) and BrHBr<sup>-</sup> ( $(0.1)^{1/2}m_{\text{Br}}$ ,  $(0.01)^{1/2}m_{\text{Br}}$ ,  $(0.001)^{1/2}m_{\text{Br}}$ ), respectively. The potential energy surfaces,  $E_{\text{c}}(r_{\text{H}}, z_{\text{H}}, r_{\text{FF}})$ , were evaluated by the Hartree–Fock method with the aug-cc-pVDZ basis set. Although the anharmonic vibrational frequencies obtained with these potentials are by no means accurate in comparison with experiments, the conclusions about the BO approximation and DBOC should not depend upon how the potentials are obtained. For accurate computational characterization of the anharmonic vibrations in FHF<sup>-</sup>, see our previous work.<sup>17</sup>

#### IV. Discussion

Table 1 attests to the remarkable accuracy of the BO approximation with the reduced hydrogen mass. The errors in the *total* energies are on the order of  $10^{-5}$  au with the largest error being only  $51 \times 10^{-6}$  au or  $11 \text{ cm}^{-1}$  (in FHF<sup>-</sup>). The errors in the *relative* energies (anharmonic vibrational frequencies) are negligibly small especially between the (000) and (100) states, which share the same effective one-dimensional potentials. The use of the bare hydrogen mass increases the errors in the total and relative energies by a factor of 2–7, but the errors are still small even in FHF<sup>-</sup> (the maximum error in the relative energies is  $99 \times 10^{-6}$  au or  $22 \text{ cm}^{-1}$ ) and smaller in ClHCl<sup>-</sup> and BrHBr<sup>-</sup>. Considering the large mass ratio ( $0.025 < \epsilon < 0.11$ ), we may conclude that the BO-like approximate separation of variables has a broad range of validity and its application should not be confined to just between electrons and nuclei ( $\epsilon \approx 0.0001$ ). The conclusion apparently disagrees with that of Dai et al.,<sup>19</sup> who applied a  $(3 + 1)$  approximate separation of variables in the four-dimensional vibrational problem of the linear OHO<sup>+</sup> fragment (as a model of H<sub>3</sub>O<sub>2</sub><sup>+</sup>) and reported poor results. The disagreement arises because, in the study of Dai et al.,<sup>19</sup> the separation was between one of the hydrogen atom’s vibrations (the antisymmetric stretch) and the other three involving both hydrogen and oxygen motion (the symmetric stretch and doubly degenerate bend) instead of a more logical separation between the vibrations of heavy and light particles.

The DBOC reduces the errors in the BO approximations uniformly by up to an order of magnitude for all states considered except for the (100) state. The so-called reduced mass errors seem to be completely erased by the DBOC, and the remaining errors are almost identical between the calculations using the reduced and bare hydrogen masses in ClHCl<sup>-</sup> and BrHBr<sup>-</sup>. The observation that the (100) state does not benefit from the DBOC and sometimes their energies deteriorate with the DBOC may be related to the fact that it is an excited state ( $\xi_1$ ) in the one-dimensional potentials, whereas the other three states all correspond to the zero-point states ( $\xi_0$ ’s) in the same potentials. This result might forewarn that, in the context of usual BO electronic structure calculations, the DBOC does not necessarily improve vibrational frequencies or may even deteriorate them, whereas it

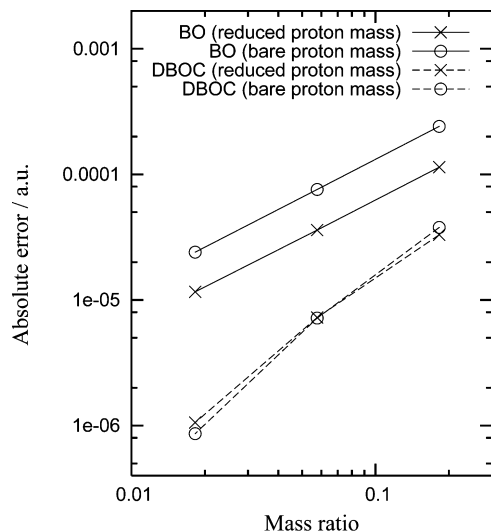


**Figure 9.** Absolute errors (in au) in the energies of the zero-point vibrational state of  $\text{ClHCl}^-$  computed in the BO approximations with and without the DBOC plotted as functions of the mass ratio  $m_{\text{H}}/m'_{\text{Cl}}$ . Both axes use logarithmic scales.

is expected to improve electronic (0–0) transition energies and zero-point vibrational energies. For higher-lying states, the BO and DBOC treatments are expected to break down as the off-diagonal BO corrections (i.e., the nonadiabatic couplings) between different hydrogen states become substantial, in particular, between the  $\zeta_0$  ( $k = 0$ ) and  $\zeta_1$  ( $k = 0$ ) states, which become degenerate as  $r_{\text{FF}} \rightarrow \infty$ . See also Mills<sup>20</sup> on the significance of DBOC in the tunneling splitting in  $\text{H-F}$  stretching vibrations in  $(\text{HF})_2$ .

Figures 8–10 demonstrate that the errors in the BO approximation scale as  $\epsilon^1$ ; the gradients of the lines connecting the points with the two smallest values of  $\epsilon$  in each log–log plot are 0.99 and 0.99 in  $\text{FHF}^-$ , 0.99 and 1.00 in  $\text{ClHCl}^-$ , and 0.84 and 0.93 in  $\text{BrHBr}^-$ , with the first of the two values corresponding to the reduced-mass calculation and the second the bare-mass calculation. The corresponding gradients of the errors in the DBOC calculations are 1.60 and 2.33 in  $\text{FHF}^-$ , 1.67 and 1.84 in  $\text{ClHCl}^-$ , and 1.94 and 2.00 in  $\text{BrHBr}^-$ , suggesting that the  $\epsilon^2$  scaling of the remaining errors after the DBOC is made. The intrinsic numerical uncertainties in the computational procedure appear to be on the order of  $10^{-6}$  au, and the reliable gradients were not obtained with smaller values of  $\epsilon$ .

Our mathematical analysis that follows indicates that the errors in the BO and DBOC calculations should scale asymptotically as  $\epsilon^1$  and  $\epsilon^2$ , respectively. Therefore, our numerical results are consistent with our analytical conclusion. Note, however, that Born and Oppenheimer<sup>1</sup> deduced that the errors inherent to the BO approximation were proportional to  $\epsilon^{5/4}$ , whereas Takahashi and Takatsuka<sup>9</sup> suggested that the correct scaling should be  $\epsilon^{3/2}$ . Our calculations and the following mathematical analysis do not support either of these conclusions,<sup>1,9</sup> but agree with the conclusions drawn from analytically solvable models by Pino and Mujica<sup>10</sup> and by Garashchuk et al.<sup>11</sup> The studies of Born and Oppenheimer and of Takahashi and Takatsuka were based on perturbation theory, whose validity had been questioned. In the following, we provide a much more transparent and concise explanation of our result (the  $\epsilon^1$  and  $\epsilon^2$  scaling of the errors in the BO and DBOC calculations, respectively) on the basis of the variational formalism of Born and Huang,<sup>21</sup> again adopting  $\text{FHF}^-$  as a representative case and using similar notation of symbols as the foregoing discussion.

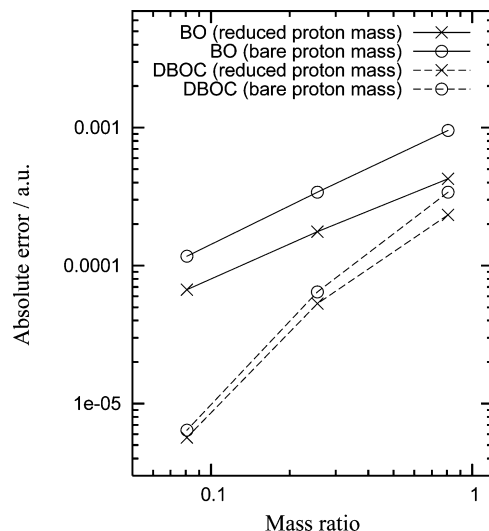


**Figure 10.** Absolute errors (in au) in the energies of the zero-point vibrational state of  $\text{BrHBr}^-$  computed in the BO approximations with and without the DBOC plotted as functions of the mass ratio  $m_{\text{H}}/m'_{\text{Br}}$ . Both axes use logarithmic scales.

The conclusions should be valid generally for most any molecules and dynamical degrees of freedom.

A vibrational wave function of  $\text{FHF}^-$  can be expanded *exactly* as

$$\Psi(\mathbf{r}_{\text{H}}, r_{\text{FF}}) = \sum_{p,k} \chi_p(\mathbf{r}_{\text{H}}; r_{\text{FF}}) \xi_{pk}(r_{\text{FF}}) \quad (28)$$

where  $\chi_p$  is the  $p$ th hydrogen wave function,  $\xi_{pk}$  is the  $k$ th fluorine wave function in the effective potential of the  $p$ th hydrogen state, and  $\mathbf{r}_{\text{H}}$  and  $r_{\text{FF}}$  are hydrogen and fluorine coordinates, respectively. The index  $p$  runs over all hydrogen wave functions, which form a complete, orthonormal set. The hydrogen and fluorine wave functions in eq 28 satisfy the following equations

$$\left\{ -\frac{1}{2m_{\text{H}}} \nabla_{\text{H}}^2 + E_e(\mathbf{r}_{\text{H}}, r_{\text{FF}}) \right\} \chi_p(\mathbf{r}_{\text{H}}; r_{\text{FF}}) = E_p(r_{\text{FF}}) \chi_p(\mathbf{r}_{\text{H}}; r_{\text{FF}}) \quad (29)$$

and

$$\sum_q \hat{H}_{pq} \xi_{qk}(r_{\text{FF}}) = E_{pk} \xi_{pk}(r_{\text{FF}}) \quad (30)$$

with

$$\hat{H}_{pq} = \delta_{pq} \left\{ -\frac{1}{2m'_{\text{F}}} \nabla_{\text{FF}}^2 + E_p(r_{\text{FF}}) \right\} - \frac{V_{pq}(r_{\text{FF}})}{2m'_{\text{F}}} - \frac{U_{pq}(r_{\text{FF}}) \cdot \nabla_{\text{FF}}}{m'_{\text{F}}} \quad (31)$$

and

$$V_{pq}(r_{\text{FF}}) = \langle \chi_p(\mathbf{r}_{\text{H}}; r_{\text{FF}}) | \nabla_{\text{FF}}^2 | \chi_q(\mathbf{r}_{\text{H}}; r_{\text{FF}}) \rangle_{\mathbf{r}_{\text{H}}} \quad (32)$$

$$U_{pq}(r_{\text{FF}}) = \langle \chi_p(\mathbf{r}_{\text{H}}; r_{\text{FF}}) | \nabla_{\text{FF}} | \chi_q(\mathbf{r}_{\text{H}}; r_{\text{FF}}) \rangle_{\mathbf{r}_{\text{H}}} \quad (33)$$

where  $E_e(\mathbf{r}_{\text{H}}, r_{\text{FF}})$  is the potential energy surface,  $E_p(r_{\text{FF}})$  is the one-dimensional effective potential of the  $p$ th hydrogen state, and  $\langle \dots \rangle_{\mathbf{r}_{\text{H}}}$  denotes an integration over the hydrogen variables.

The BO and DBOC treatments amount to retaining only one dominant contribution in the summation of eq 28. In other words, they correspond to setting all off-diagonal elements of  $\hat{H}_{pq}$  in eq 31 to zero. Defining approximate, diagonal Hamiltonians by

$$\hat{H}_{pq}^{\text{BO}} = \delta_{pq} \left\{ -\frac{1}{2m_{\text{F}}'} \nabla_{\text{FF}}^2 + E_p(r_{\text{FF}}) \right\} \quad (34)$$

$$\hat{H}_{pq}^{\text{DBOC}} = \hat{H}_{pq}^{\text{BO}} - \delta_{pq} \frac{V_{pq}(r_{\text{FF}}) + 2U_{pq}(r_{\text{FF}}) \cdot \nabla_{\text{FF}}}{2m_{\text{F}}'} \quad (35)$$

the BO and DBOC results are obtained by solving the following uncoupled equations:

$$\hat{H}_{pp}^{\text{BO}} \xi_{pk}^{\text{BO}}(r_{\text{FF}}) = E_{pk}^{\text{BO}} \xi_{pk}^{\text{BO}}(r_{\text{FF}}) \quad (36)$$

$$\hat{H}_{pp}^{\text{DBOC}} \xi_{pk}^{\text{DBOC}}(r_{\text{FF}}) = E_{pk}^{\text{DBOC}} \xi_{pk}^{\text{DBOC}}(r_{\text{FF}}) \quad (37)$$

respectively.

Let us analyze the asymptotic polynomial dependence on  $\epsilon$  of the various factors entering these equations.  $E_p(r_{\text{FF}})$  in eq 29 is an effective potential for the F–F stretching motion. Since eq 29 does not depend on the reduced fluorine mass ( $m_{\text{F}}'$ ),  $E_p(r_{\text{FF}})$  is independent of the mass ratio  $\epsilon$ ; in other words,  $E_p(r_{\text{FF}})$  scales as  $\epsilon^0$ . When the reduced hydrogen mass ( $m_{\text{H}}'$ ) is used in eq 29,  $E_p(r_{\text{FF}})$  depends very weakly on  $m_{\text{F}}'$ , but its effect on this scaling discussion is negligible. A quantum (transition energy) of the fluorine atoms' vibration in the BO approximation,  $E_{p0}^{\text{BO}} - E_{p1}^{\text{BO}}$ , scales as  $\epsilon^{1/2}$ . This is based on the assumption that  $E_p(r_{\text{FF}})$  is approximately harmonic and on the fact that a vibrational quantum of a harmonic oscillator shows the inverse-square-root dependence on the reduced mass. It should be cautioned that a different assumption on the shape of  $E_p(r_{\text{FF}})$  (e.g., the particle in a box) leads to different scaling behavior.

The matrix representation of  $\hat{H}_{pp}^{\text{BO}}$  in the basis of the eigenfunctions,  $\{\xi_{pk}^{\text{BO}}\}$ , is diagonal with the diagonal elements being equal to  $E_{pk}^{\text{BO}}$  (eq 36). Considering just two fluorine atoms' vibrational states ( $k = 0$  and 1) (not to be confused with the angular momentum) in the single,  $p$ th hydrogen state, it has the structure

$$\mathbf{H}_{pp}^{\text{BO}} = \begin{pmatrix} E_{p0}^{\text{BO}} & 0 \\ 0 & E_{p1}^{\text{BO}} \end{pmatrix} \quad (38)$$

where  $E_{p0}^{\text{BO}} < E_{p1}^{\text{BO}}$  is assumed. In the same basis, the matrix representation of  $\hat{H}_{pp}^{\text{DBOC}}$  is no longer diagonal as the DBOC adds the nonconstant corrections to  $\hat{H}_{pp}^{\text{BO}}$ , and therefore,  $\{\xi_{pk}^{\text{BO}}\}$  is not an eigenfunction of  $\hat{H}_{pp}^{\text{DBOC}}$  (eqs 35 and 37). Hence, the matrix now has the form

$$\mathbf{H}_{pp}^{\text{DBOC}} = \begin{pmatrix} E_{p0}^{\text{BO}} + e_{p0,p0} & e_{p0,p1} \\ e_{p1,p0} & E_{p1}^{\text{BO}} + e_{p1,p1} \end{pmatrix} \quad (39)$$

with

$$e_{pk,pl} = -\frac{\langle \xi_{pk}^{\text{BO}} | V_{pp} | \xi_{pl}^{\text{BO}} \rangle_{r_{\text{FF}}}}{2m_{\text{F}}'} \quad (40)$$

because  $U_{pp} = 0$ . The corrections ( $e_{pk,pl}$ ) to individual matrix elements scale as  $\epsilon^1$  because of the  $1/m_{\text{F}}'$  factor in eq 40. Using  $(1+x)^{1/2} \approx 1+x/2$ , we find that the eigenvalues of the  $2 \times 2$  matrix  $\mathbf{H}_{pp}^{\text{DBOC}}$  are approximately

$$E_{p0}^{\text{BO}} + e_{p0,p0} - \frac{e_{p0,p1}e_{p1,p0}}{E_{p1}^{\text{BO}} - E_{p0}^{\text{BO}}} \quad (41)$$

and

$$E_{p1}^{\text{BO}} + e_{p1,p1} + \frac{e_{p0,p1}e_{p1,p0}}{E_{p1}^{\text{BO}} - E_{p0}^{\text{BO}}} \quad (42)$$

These eigenvalues are the sums of the corresponding BO energies ( $E_{p0}^{\text{BO}}$  and  $E_{p1}^{\text{BO}}$ ), the leading-order corrections ( $e_{p0,p0}$  and  $e_{p1,p1}$ ), the second leading-order corrections, and so forth. The leading-order corrections scale as  $\epsilon^1$ . The numerators in the second leading-order corrections are proportional to  $\epsilon^2$ , whereas the denominators scale as  $\epsilon^{1/2}$  because the energy difference  $E_{p1}^{\text{BO}} - E_{p0}^{\text{BO}}$  corresponds to a quantum of the fluorine atoms' vibration. Overall, the second leading-order corrections are proportional to  $\epsilon^{3/2}$ . Therefore, the differences between the BO and DBOC energies scale as  $\epsilon^1$  and the errors (from the exact values) in the BO energies should thus depend linearly on the mass ratio. If the DBOC is made in the first-order perturbation approximation of eq 16, only the leading-order corrections ( $e_{p0,p0}$  and  $e_{p1,p1}$ ) are added to the BO energies. The second leading-order contributions, which arise from the off-diagonal elements in the matrix  $\mathbf{H}_{pp}^{\text{DBOC}}$ , are not included in the first-order perturbation treatment of DBOC, which, therefore, has the errors on the order of  $\epsilon^{3/2}$ .

Switching the basis to  $\{\xi_{pk}^{\text{DBOC}}\}$ , we can bring the matrix representation of  $\hat{H}_{pp}^{\text{DBOC}}$  to a diagonal form. What is approximated in this representation are the couplings across different hydrogen states. The matrix representation of the exact Hamiltonian  $\hat{H}$  has nonzero off-diagonal elements in the basis of  $\{\xi_{pk}^{\text{DBOC}}\}$  and looks like

$$\mathbf{H}_{pq} = \begin{pmatrix} E_{p0}^{\text{DBOC}} & e'_{p0,q0} \\ e'_{q0,p0} & E_{q0}^{\text{DBOC}} \end{pmatrix} \quad (43)$$

in the simple case of two hydrogen states ( $E_{q0}^{\text{DBOC}} > E_{p0}^{\text{DBOC}}$ ), where  $e'_{p0,q0}$  vanishes when  $p = q$  and otherwise

$$e'_{pk,ql} = -\frac{\langle \xi_{pk}^{\text{DBOC}} | V_{pq} + 2U_{pq} \cdot \nabla_{\text{FF}} | \xi_{ql}^{\text{DBOC}} \rangle_{r_{\text{FF}}}}{2m_{\text{F}}'} \quad (44)$$

The eigenvalues are approximately

$$E_{p0}^{\text{DBOC}} - \frac{e'_{p0,q0}e'_{q0,p0}}{E_{q0}^{\text{DBOC}} - E_{p0}^{\text{DBOC}}} \quad (45)$$



**TABLE 2: Asymptotic Polynomial Dependence of Errors in the Various Approximate Solutions of the Schrödinger Equation on the Mass Ratio  $\epsilon$  ( $\epsilon \ll 1$ )**

approximation	energy expression in this article	error
light particle only	$E_{eH}$ or $E_p$ (at its minimum)	$\epsilon^{1/2}$
BO	$E^{BO}$ , $\bar{E}^{BO}$ , or $E_{p0}^{BO}$	$\epsilon^1$
DBOC (perturbation)	$\bar{E}^{DBOC}$ or $E_{p0}^{DBOC} + e_{p0,p0}$	$\epsilon^{3/2}$
DBOC (variation)	$E^{DBOC}$ , $\bar{E}^{DBOC}$ , or $E_{p0}^{DBOC}$	$\epsilon^2$

and

$$E_{q0}^{DBOC} + \frac{e'_{p0,q0}e'_{q0,p0}}{E_{q0}^{DBOC} - E_{p0}^{DBOC}} \quad (46)$$

The last terms in the above two expressions are the leading-order differences in energy between DBOC and exact treatments and are the measures of the errors in the energies after the DBOC is made variationally. Their numerators scale as  $\epsilon^2$  because of the  $1/m_F$  dependence of  $e'_{pk,ql}$  (eq 44). The denominators correspond to the energy differences between two hydrogen states and are independent of the halogen mass; they scale as  $\epsilon^0$ . Consequently, these leading-order corrections to the DBOC energies and hence the errors in the DBOC energies are asymptotically proportional to  $\epsilon^2$ .

Table 2 summarizes the conclusion of the analysis, which applies to both reduced- and bare-mass calculations. The errors in the energies obtained by the BO calculations are asymptotically proportional to  $\epsilon^1$ . When DBOC is applied in the first-order perturbation approximation of eq 16, the errors reduce to  $\epsilon^{3/2}$ . The errors in the complete DBOC calculations (using the “adiabatic” potential energy surfaces and variationally determining the wave function for these surfaces) scale as  $\epsilon^2$ . When the F–F stretch vibrations are altogether neglected and  $E_p(r_{FF})$  is minimized by varying  $r_{FF}$ , the energy suffers from much greater errors that are proportional to  $\epsilon^{1/2}$  (the zero-point vibrational energy of the F–F stretch). While these conclusions are deduced taking  $2 \times 2$  matrices as examples, they are valid for any number of the hydrogen atom’s and fluorine atoms’ vibrational states. They should also be true for the usual BO separation between electrons and nuclei and DBOC in electronic structure theory insofar as the coupling of rotational motion from the rest is negligible. The  $\epsilon^{3/2}$  and  $\epsilon^2$  dependence of the remaining errors in DBOC treatments is also consistent with the findings of Pino and Mujica<sup>10</sup> and Garashchuk et al.,<sup>11</sup> respectively, for analytically solvable models.

## V. Conclusions

The errors in the BO-like approximate separation of variables between heavy- and light-particle vibrations have been found to be remarkably small (on the order of  $10^{-5}$  au) in spite of the large mass ratio  $\epsilon \approx 0.1$ . When the bare hydrogen mass is used instead of reduced hydrogen mass

and, therefore, the translational degrees of freedom are not correctly decoupled from the others, the errors increase by a factor of 2–7, but still remain to be relatively small overall. This encourages us to broaden the application domain of BO-like approximate separation of variables to dimensions less explored by this technique. The DBOC has also proven effective in systematically reducing these already small errors to varied degrees except for the states that are excited in the halogen–halogen stretch. The exact cause of the latter is unclear but is probably related to the fact that these states are not the lowest states of the effective one-dimensional potentials. The so-called “reduced mass errors” in the bare-mass calculations are almost completely erased by the DBOC. Our numerical and analytical results have revised the previous conclusions by Born and Oppenheimer<sup>1</sup> and Takahashi and Takatsuka<sup>9</sup> on the asymptotic polynomial dependence of the errors in the BO treatments on the mass ratio  $\epsilon$ . The correct dependence of errors has been found to be  $\epsilon^1$ ,  $\epsilon^{3/2}$ , and  $\epsilon^2$  in the BO, DBOC (perturbation), and DBOC (variational) treatments, respectively.

**Acknowledgment.** This work was financially supported by the Department of Energy (DE-FG02-04ER15621), the National Science Foundation (CHE-0844448), and the American Chemical Society Petroleum Research Fund (48440-AC6). S.H. is a Camille Dreyfus Teacher-Scholar.

## References and Notes

- (1) Born, M.; Oppenheimer, R. *Ann. Phys.* **1927**, *84*, 457.
- (2) Tachikawa, M.; Mori, K.; Nakai, H.; Iguchi, K. *Chem. Phys. Lett.* **1998**, *290*, 437.
- (3) Nakai, H.; Sodeyama, K.; Hoshino, M. *Chem. Phys. Lett.* **2001**, *345*, 118.
- (4) Webb, S. P.; Iordanov, T.; Hammes-Schiffer, S. *J. Chem. Phys.* **2002**, *117*, 4106.
- (5) Cafiero, M.; Bubin, S.; Adamowicz, L. *Phys. Chem. Chem. Phys.* **2003**, *5*, 1491.
- (6) Bochevarov, A. D.; Valeev, E. F.; Sherrill, C. D. *Mol. Phys.* **2004**, *102*, 111.
- (7) Nakai, H. *Int. J. Quantum Chem.* **2007**, *107*, 2849.
- (8) Lohr, L. L.; Sloboda, R. J. *J. Phys. Chem.* **1981**, *85*, 1332.
- (9) Takahashi, S.; Takatsuka, K. *J. Chem. Phys.* **2006**, *124*, 144101.
- (10) Pino, R.; Mujica, V. *J. Phys. B: At. Mol. Opt. Phys.* **1998**, *31*, 4537.
- (11) Garashchuk, S.; Light, J. C.; Rassolov, V. A. *Chem. Phys. Lett.* **2001**, *333*, 459.
- (12) Handy, N. C.; Lee, A. M. *Chem. Phys. Lett.* **1996**, *252*, 425.
- (13) Kutzelnigg, W. *Mol. Phys.* **1997**, *90*, 909.
- (14) Kutzelnigg, W. *Mol. Phys.* **2007**, *105*, 2627.
- (15) Skone, J. H.; Pak, M. V.; Hammes-Schiffer, S. *J. Chem. Phys.* **2005**, *123*, 134108.
- (16) Sumner, I.; Iyengar, S. S. *J. Phys. Chem. A* **2007**, *111*, 10313.
- (17) Hirata, S.; Yagi, K.; Perera, S. A.; Yamazaki, S.; Hirao, K. *J. Chem. Phys.* **2008**, *128*, 214305.
- (18) Davidson, E. R. *J. Comput. Phys.* **1975**, *17*, 87.
- (19) Dai, J.; Bačić, Z.; Huang, X. C.; Carter, S.; Bowman, J. M. *J. Chem. Phys.* **2003**, *119*, 6571.
- (20) Mills, I. M. *J. Phys. Chem.* **1984**, *88*, 532.
- (21) Born, M.; Huang, K. *Dynamical Theory of Crystal Lattices*; Oxford University Press: New York, 1954.

JP903375D